Luminescence and Energy Transfer in $Eu^{2?+?}$ and $Mn^{2?+?}$ Co-doped $Ca_2P_2O_7$ for White Light-Emitting Diodes

Zhendong Hao, Zhaogang Nie, Song Ye, Ruixia Zhong, Xia Zhang, Li Chen, Xinguang Ren, Shaozhe Lu, Xiao-jun Wang and Jiahua Zhang

J. Electrochem. Soc. 2008, Volume 155, Issue 8, Pages H606-H610.
doi: 10.1149/1.2943412

Journal of The Electrochemical Society, **155** (8) H606-H610 (2008)
0013-4651/2008/155(8)/H606/5/$23.00 © The Electrochemical Society

Luminescence and Energy Transfer in Eu^{2+} and Mn^{2+} Co-doped $Ca_2P_2O_7$ for White Light-Emitting Diodes

Zhendong Hao,[a,b,c] Zhaogang Nie,[a,b,c] Song Ye,[a,b,c] Ruixia Zhong,[a,b,c] Xia Zhang,[b] Li Chen,[b] Xinguang Ren,[b] Shaozhe Lu,[b] Xiao-jun Wang,[b,d] and Jiahua Zhang[b,*,z]

[a]*Key Laboratory of Excited State Processes and* [b]*Changchun Institute of Optics, Fine Mechanics and Physics (CIOMP), Chinese Academy of Sciences, Changchun 130033, China*
[c]*Graduate School of Chinese Academy of Sciences, Beijing, 100039, China*
[d]*Department of Physics, Georgia Southern University, Statesboro, Georgia 30460, USA*

Eu^{2+} and Mn^{2+} co-doped α- and β-$Ca_2P_2O_7$ are prepared by solid-state reaction. An orange emission band originating from the $^4T_1(^4G)$-$^6A_1(^6S)$ transition of Mn^{2+} is observed in both phases upon UV excitation through energy transfer from Eu^{2+} to Mn^{2+}. Photoluminescence and energy transfer in α-$Ca_2P_2O_7$:Eu^{2+}, Mn^{2+} are investigated as a function of Mn^{2+} concentrations. The energy transfer rates are calculated based on the analysis of the luminescence dynamical process as well as fluorescence lifetime measurements. The intensity ratios of the orange to blue band as a function of Mn^{2+} concentrations are also calculated and the results are in good agreement with that obtained directly from emission spectra. A white light emitting diode (LED) fabricated through the integration of a GaN near-UV chip and two phosphor blends (α-$Ca_2P_2O_7$:Eu^{2+}, Mn^{2+} blue-orange phosphor and Ba_2SiO_4:Eu^{2+} green phosphor) into a single package shows a warm white light of 3797 K correlated color temperature, a good color rendering index (CRI) of 84, and a luminescent efficiency of 11 lm/W with color coordinates of $x = 0.39$, $y = 0.40$. Moreover, the CRI can be improved to 94 by using blue $Ca^2(PO4)_3Cl$:Eu^{2+} phosphor added to the two phosphor blends.
 [DOI: 10.1149/1.2943412]

Manuscript submitted March 18, 2008; revised manuscript received May 22, 2008. Available electronically June 26, 2008.

The light-emitting diodes (LED)-based white light sources have received increasing interest in recent years for their promising applications on illuminations with advantages over the existing incandescent and halogen lamps in power efficiency, reliability, long lifetime, and environmental protection.[1-4] The conventional way to realize white LED involves combining a blue LED with a yellow-emitting $Y_3Al_5O_{12}$:Ce^{3+}(YAG) phosphor. The white light is generated by additive color mixing of the blue light emitted by the blue LED and the yellow light emitted by the YAG phosphors. This method is relatively easy to perform and the device has been commercialized. However, for general illumination, there are several problems present with this type of white LED: white-emitting color changes with input power, a low color rendering index (CRI) due to two-color mixing, and a low reproducibility due to strong dependence of white color quality on an amount of phosphor.

To solve these problems, the white LED has been suggested to fabricate blue, green, and red phosphors with a near-UV chip. This technology can thus provide a higher CRI and high tolerance to the UV chip's color variation in the respect that the white color is generated only by phosphors. The current phosphor materials suitable for near-UV LEDs are $BaMgAl_{10}O_{17}$:Eu^{2+} for blue, ZnS:Cu^+,Al^{3+} for green, and Y_2O_2S:Eu^{3+} for red.[5] However, the absorption band of Eu^{3+} predominating at 394 nm in most matrices can hardly accommodate to an even smaller extent with the excursion of the emission band of near-UV chip. What is more, their stability is not high enough, and their decomposition products (such as sulfide gas) are harmful to the environment. Therefore, the development of efficient orange or red phosphors that can be excited by around 400 nm irradiation is still a key technology for achieving the tricolor white LED lighting systems.[6]

Calcium pyrophosphate ($Ca_2P_2O_7$) has extensive applications in the fields of luminescence and biomaterials due to its improved optical and biological characteristics.[7] The blue-orange $Ca_2P_2O_7$:Eu^{2+}, Mn^{2+} phosphor is also a good phosphor for lamps through the energy transfer from Eu^{2+} to Mn^{2+}.[8] However, most of them concern beta phase calcium pyrophosphate. In our previous work,[9] we have demonstrated a white LED fabricated through combining a GaN near-UV chip with two phosphor blends of the blue-orange α-$Ca_2P_2O_7$:Eu^{2+}, Mn^{2+} and a green Ba_2SiO_4:Eu^{2+} phosphor.[10] When the forward-bias current is 20 mA, the Commission Internationale de I'Eclairage (CIE) coordinates are $x = 0.27$, $y = 0.30$, the CRI is 78, the luminous efficiency is 9 lm/W, and the correlated color temperature (T_c) is 10,465 K. The results of CIE coordinates and the correlated color temperature indicate that the LED emission shows bluish white due to the weak spectral content of the orange light.

In this paper, we report on the preparation and photoluminescence properties (PL) of $Ca_2P_2O_7$:Eu^{2+}, Mn^{2+} in detail. The energy transfers in α-$Ca_2P_2O_7$:Eu^{2+}, Mn^{2+} are also roundly investigated. By tuning the weight ratio of α-$Ca_2P_2O_7$:Eu^{2+}, Mn^{2+} phosphor and Ba_2SiO_4:Eu^{2+} phosphor, the improvement of white light with good color rendering and warm white light have been realized.

Experimental

Synthesis.— All the compounds were synthesized by solid-state reaction. The starting materials, analytical grade $CaHPO_4$, $MnCO_3$, $(NH_4)_2HPO_4$, and Eu_2O_3, were homogenized by an agate mortar, pestled for 1 h, and placed in a crucible with a lid. The crucible was preheated at 600°C for 1 h, cooled down, ground, and put into the crucible again, which was buried by carbon sticks and sintered at 1150°C for β-$Ca_2P_2O_7$:Eu^{2+}, Mn^{2+} and 1250°C for α-$Ca_2P_2O_7$:Eu^{2+}, Mn^{2+}, respectively, for 2 h in a CO reducing atmosphere. The concentration of Eu^{2+} was fixed at 1 and 4 mol %, while the Mn^{2+} concentrations were varied from 4 to 14 mol %. The green Ba_2SiO_4:0.03Eu^{2+} phosphor for mixing with α-$Ca_2P_2O_7$:Eu^{2+}, Mn^{2+} was synthesized by the process as described in Ref. 10.

Characterization.— The structure of sintered samples was identified by an X-ray powder diffractometer (Rigaku D/M AX-2500 V), operating at 40 kV and 20 mA and using Cu Kα radiation (λ = 1.54056 Å). A step size of 0.02°(2θ) was used with a scanning speed of 4°/min. The measurements of PL and photoluminescence excitation (PLE) spectra were performed by using a Hitachi F4500 spectrometer equipped with a 150 W xenon lamp under a working voltage of 700 V. The excitation and emission slits were both set at 2.5 nm. In fluorescence lifetime measurements, the third harmonic (355 nm) of a Nd-doped yttrium aluminum garnet laser (Spectra-Physics, GCR 130) was used as an excitation source, and the signals were detected with a Tektronix digital oscilloscope (TDS 3052). The

* Electrochemical Society Active Member.
z E-mail: zhangjh@ciomp.ac.cn

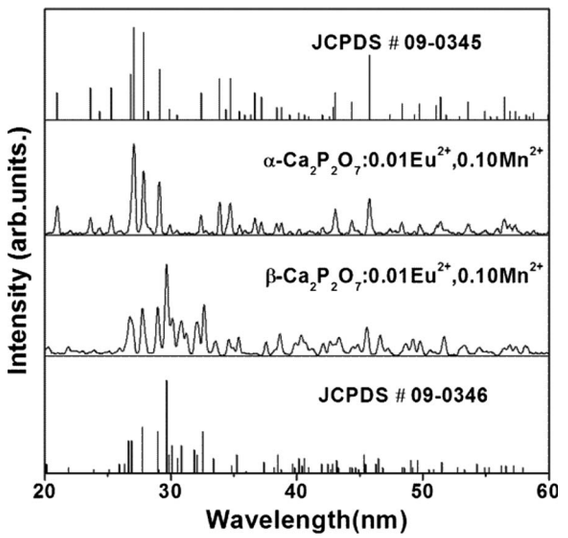

Figure 1. XRD patterns of α- and β-$Ca_2P_2O_7$:0.01Eu^{2+}, 0.10Mn^{2+}. The standard XRD patterns of JCPDS File no. 09–0345 (monoclinic phase) and JCPDS File no. 09–0346 (tetragonal phase) are also shown.

chromaticity coordinates and the CRI, as well as the correlated color temperature (T_c) in Kelvin of the fabricated white LED, were obtained using a PR-705 SpectraScan spectroradiometer. All the measurements were performed at room temperature.

Results and Discussion

Phase transition.— Figure 1 shows the X-ray diffraction (XRD) patterns of α- and β-$Ca_2P_2O_7$:0.01Eu^{2+}, 0.10Mn^{2+} phosphor sintered at 1250 and 1150°C, respectively. It can be seen that all the peaks of α- and β-$Ca_2P_2O_7$:0.01Eu^{2+}, 0.12Mn^{2+} coincide well with the monoclinic phase (JCPDS no. 09–0345) and tetragonal phase (JCPDS no. 09–0346), respectively, and no impurity peaks can be detected in the XRD analysis, indicating that the obtained samples are all single phase.

Photoluminescent properties.— Figure 2 illustrates the PLE and PL spectra of α- and β-$Ca_2P_2O_7$:0.01Eu^{2+}, 0.10Mn^{2+} phosphors. The emission spectra of both the samples under 330 nm excitation show a blue emission band and an orange emission band, which are

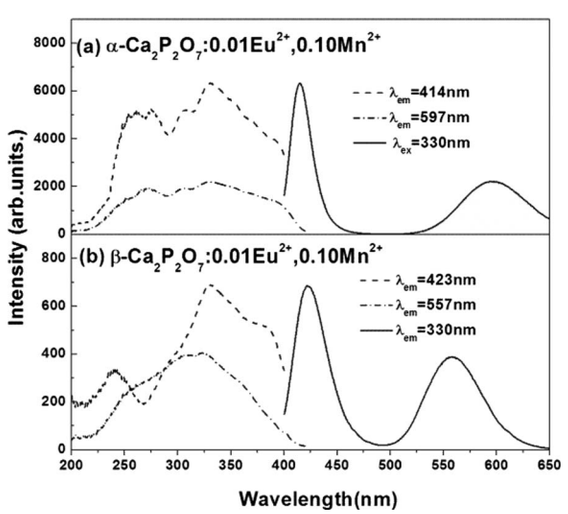

Figure 2. PL and PLE spectra of α- and β-$Ca_2P_2O_7$:0.01Eu, 0.10Mn.

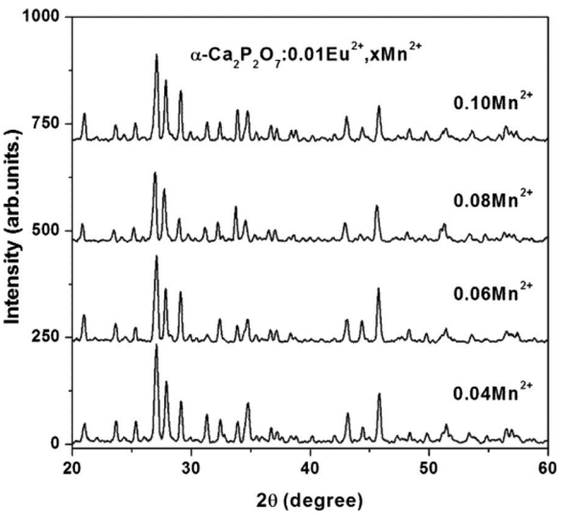

Figure 3. XRD patterns of α-$Ca_2P_2O_7$:0.01Eu^{2+}, $x$$Mn^{2+}$ sintered at 1250°C.

originated from the 5d–4f transition of Eu^{2+} and the $^4T_1(^4G)$–$^6A_1(^6S)$ transition of Mn^{2+}, respectively. With the phase transformation from β to α, it is observed that the blue emission band of Eu^{2+} slightly shifts toward the blue side from 419 to 416 nm along with increasing emission intensity and narrowing bandwidth, while the orange emission peak clearly shifts toward the red side from 567 to 595 nm. The bond length (R) of Ca–O in α-$Ca_2P_2O_7$ is 2.53 vs 2.73 Å in β-$Ca_2P_2O_7$, which should increase the crystal field splitting and the redshift of the Mn^{2+} emission band. The relationship between crystal field splitting and bond length is well known in octahedral complexes, where there is an R^{-5} relationship.[11-13] The weak blueshift of the blue emission of Eu^{2+} may be the result of the polyhedral distortion in crystal structure.

All the PLE spectra are composed of several bands, which originate from the parity allowed $4f^7$–$4f^65d$ transitions of Eu^{2+} ions. In Fig. 2a, it is found that the PLE spectrum monitoring the orange emission of the Mn^{2+} (dashed-dot line) is similar to that monitoring the blue emission of Eu^{2+} (dashed line), demonstrating the existence of energy transfer from Eu^{2+} to Mn^{2+} in α-$Ca_2P_2O_7$. However, in β-$Ca_2P_2O_7$:0.01Eu^{2+}, 0.10Mn^{2+}, as shown in Fig. 2b, the PLE spectra of Mn^{2+} (dashed-dot line) are different from that of Eu^{2+} (dash line), indicating the different energy transfer efficiency from Eu^{2+} to Mn^{2+} at different excitation wavelengths. In addition, the PLE band in α-$Ca_2P_2O_7$:0.01Eu^{2+}, 0.10Mn^{2+} extends into 430 nm, covering almost the full near-UV region, while the PLE band in β-$Ca_2P_2O_7$:0.01Eu^{2+}, 0.10Mn^{2+} becomes suddenly weak near 400 nm. Therefore, α-$Ca_2P_2O_7$:Eu^{2+}, Mn^{2+} can be used as a promising phosphor with an intense orange component applied to white LEDs technology, due to its strong luminescence and excellent profile of the PLE spectra.

Crystal structure of α-$Ca_2P_2O_7$:Eu^{2+}, Mn^{2+}.— Figure 3 depicts the XRD patterns of α-$Ca_2P_2O_7$:Eu^{2+}, Mn^{2+} phosphors with various Mn^{2+} concentrations. It is found that the XRD patterns are almost unchanged with increasing the Mn^{2+} ion content. It is also shown that the optimal sintering temperature for α-$Ca_2P_2O_7$:Eu^{2+}, Mn^{2+} is 1250°C.

Energy transfer between Eu^{2+} and Mn^{2+} in α-$Ca_2P_2O_7$.— In our previous work,[9] the excitation and emission spectra of α-$Ca_2P_2O_7$:Eu^{2+}, α-$Ca_2P_2O_7$:Mn^{2+}, and α-$Ca_2P_2O_7$:Eu^{2+}, Mn^{2+} are presented in a comparable way. By comparing the PL spectra of $Ca_2P_2O_7$:Eu^{2+} with the PLE spectra of $Ca_2P_2O_7$:Mn^{2+}, it reveals a significant spectral overlap between the emission band of Eu^{2+} centered at 416 nm and the PLE band of Mn^{2+} around 406 nm, indicat-

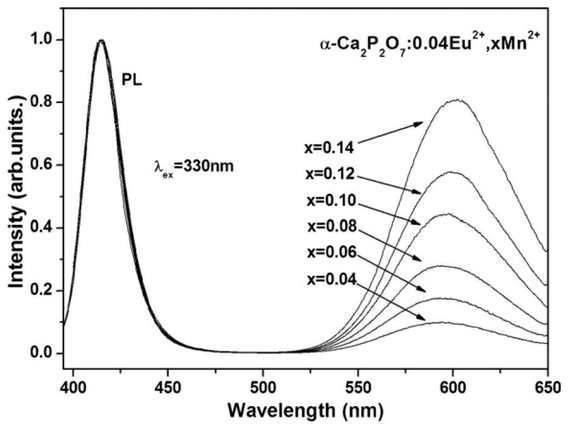

Figure 4. PL spectra (λ_{ex} = 330 nm) of α-$Ca_2P_2O_7$:0.04Eu^{2+}, $x$$Mn^{2+}$.

ing that there may be an energy transfer from Eu^{2+} to Mn^{2+} in the α-$Ca_2P_2O_7$ host. To learn more about the dynamical process of the energy transfer between Eu^{2+} and Mn^{2+} in α-$Ca_2P_2O_7$, the samples with different Mn^{2+} concentrations and a fixed Eu^{2+} concentration of 4 mol % were prepared. Figure 4 shows the emission spectra (λ_{ex} = 330 nm) of these samples, in which the intensities of the blue bands were normalized. One can see that the intensity ratio of the orange band to the blue band grows with increasing Mn^{2+} concentrations. This growth is related to the growth of the energy transfer rates from Eu^{2+} to Mn^{2+}, resulting in a reduction of the lifetimes of the blue fluorescence of Eu^{2+}.

The fluorescence lifetimes of Eu^{2+}(τ_1) and Mn^{2+}(τ_2) are both represented in Fig. 5. The reduction of the lifetimes for Eu^{2+} with increasing Mn^{2+} concentrations is observed, demonstrating the effect of energy transfer from Eu^{2+} to Mn^{2+}.[14,15] The lifetime of the orange fluorescence of Mn^{2+} remains nearly unchanged, indicating the nonexistence of Mn^{2+} concentration quenching within the range of Mn^{2+} concentrations of interest in this work.

The energy transfer rates (W_{Eu-Mn}) can be obtained using the following equation

$$W_{Eu-Mn} = \frac{1}{\tau_1} - \frac{1}{\tau_0} \qquad [1]$$

where τ_1 and τ_0 are fluorescence lifetimes of Eu^{2+} with and without codoping of Mn^{2+}, respectively. Figure 6 shows the dependence of

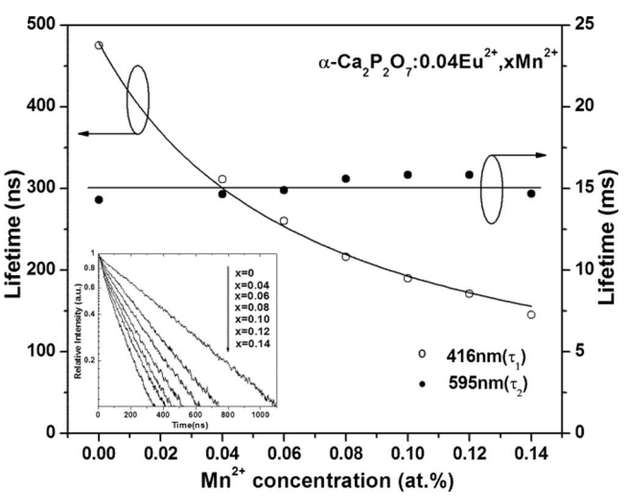

Figure 5. Lifetimes of Eu^{2+} and Mn^{2+} in α-$Ca_2P_2O_7$:0.04Eu^{2+}, $x$$Mn^{2+}$.

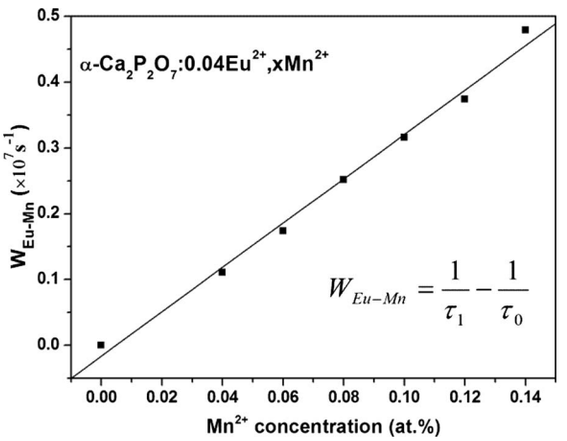

Figure 6. Dependence of the energy transfer rate (W_{Eu-Mn}) in α-$Ca_2P_2O_7$:0.04Eu^{2+}, $x$$Mn^{2+}$ on Mn^{2+} content x.

the energy transfer rate (W_{Eu-Mn}) on Mn^{2+} concentrations. It carries out a linear dependence. We also observed in lifetime measurements that each of the blue fluorescence decay patterns for different Mn^{2+} concentrations can be close to a single exponential function though with less deviation from linear, as shown in the insets of Fig. 5. These behaviors indicate that the energy diffusion among donors (Eu^{2+}) is sufficiently faster than energy transfer to acceptors (Mn^{2+}).[16]

Intensity ratios of Mn^{2+} orange to Eu^{2+} blue emission as a function of Mn^{2+} concentration.— Based on energy transfer, the dependences of the intensity ratio of the orange to blue emissions with Mn^{2+} concentrations are considered in this work. The ratio can be written as

$$\frac{S_R}{S_B} = \frac{W_{Eu-Mn}\tau_2\gamma_2}{\gamma_1} \qquad [2]$$

where γ_1 and γ_2 are radiative rates of Eu^{2+} and Mn^{2+}, respectively, which are independent of Mn^{2+} concentrations. W_{Eu-Mn} has been calculated according to Eq. 1. τ_2 has been measured and represented in Fig. 5. Therefore, the intensity ratios S_R/S_B at various Mn^{2+} concentrations can be calculated using Eq. 2 and scaled to the maximum, as presented in Fig. 7. For comparison, the intensity ratios

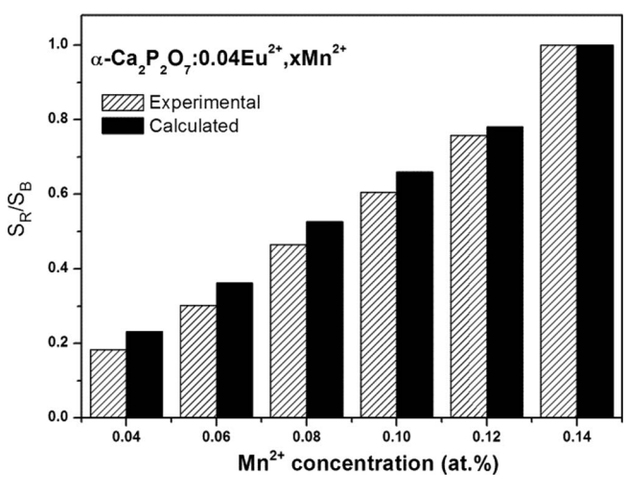

Figure 7. Calculated and experimental ratios (S_R/S_B) of the orange band to the blue band at different Mn^{2+} concentrations. The ratios are scaled to the maximum.

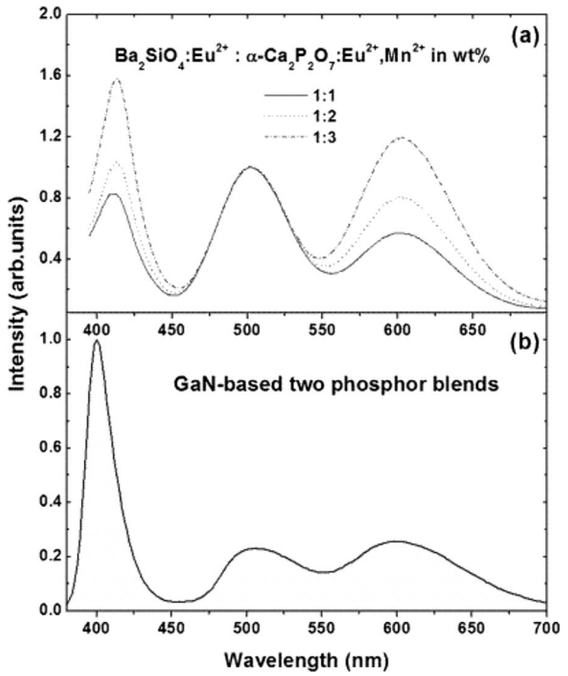

Figure 8. (a) PL spectra of the blend phosphors of α-$Ca_2P_2O_7$:0.04Eu^{2+}, 0.12Mn^{2+}, and Ba_2SiO_4:0.03Eu^{2+} phosphors mix in different ratios and (b) the UV-pumped white LED with the blend phosphors of α-$Ca_2P_2O_7$:0.04Eu^{2+}, 0.12Mn^{2+} and Ba_2SiO_4:0.03Eu^{2+} in the ratio of 3:1 under the forward-bias currents of 20 mA.

obtained directly from the emission spectra are also given in Fig. 7. The calculated data are in good agreement with the experimental ones.

White LED by using α-$Ca_2P_2O_7$:Eu^{2+}, Mn^{2+}.— To apply to the field of solid-state lighting, the white LEDs are fabricated through combining a near-UV chip with two phosphor blends of the green-poor α-$Ca_2P_2O_7$:0.04Eu^{2+}, 0.12Mn^{2+} and a green Ba_2SiO_4:0.03Eu^{2+} phosphor.[10] To get the warm white light (low color temperature) and high CRI, required for general illumination, blend phosphors with different ratios are carried out. The PL spectra shown in Fig. 8a are composed of three emission colors: a blue band of 416 nm, a green band of 505 nm, and an orange band of 595 nm. As an increase of the mixture ratio of α-$Ca_2P_2O_7$:0.04Eu^{2+}, 0.12Mn^{2+} to Ba_2SiO_4:0.03Eu^{2+}, the blue and the orange bands are increased compared with the green bands which are normalized. The ratio of 1:3 is chosen to combine with a GaN near-UV chip to fabricate warm white LEDs. The PL spectrum of the fabricated LEDs under 20 mA forward-bias currents is shown in Fig. 8b. Obviously, the spectrum exhibits the emission colors of the two phosphor blends. The asymmetry of the 400 nm band is caused by overlapping with the 416 nm emission band of the α-$Ca_2P_2O_7$:0.04Eu^{2+}, 0.12Mn^{2+} phosphor.

The chromaticity coordinates on CIE 1931 of this white LED are shown in Table I. When the forward-bias current is 20 mA, the CIE coordinates are $x = 0.39$, $y = 0.40$, the CRI is 84, the correlated color temperature (T_c) is 3797 K, and the luminous efficiency is 11 lm/W. With an increase in the applied currents, the CIE chromaticity coordinates shift slightly in direction because of the weak contribution of UV light to the CIE chromaticity coordinates of white light, indicating that the UV LED has a higher color stability than the blue chip LEDs.[17] Moreover, to improve the CRI, we also combined a near-UV chip with three phosphor blends of the blue $Ca_2(PO4)_3Cl:Eu^{2+}$,[18] blue–orange α-$Ca_2P_2O_7$:0.04Eu^{2+}, 0.12Mn^{2+}, and green Ba_2SiO_4:0.03Eu^{2+} phosphor. The PL spectrum of the fabricated LEDs under 20 mA forward-bias currents is shown in Fig. 9. It exhibits four bands at 395, 450, 505, and 595 nm, which combine to generate white light to the naked eye. The CIE coordinates are $x = 0.30$, $y = 0.32$, and the color temperature is 6570 K. The CRI of 94 is obtained.

Table I. Optical properties of the fabricated UV-pumped white LED with α-$Ca_2P_2O_7$:0.04Eu^{2+}, 0.12Mn^{2+}, and Ba_2SiO_4:0.03Eu^{2+} phosphors in the ratio of 3:1 with increasing forward-bias currents.

Current (mA)	CIE(x)	CIE(y)	CCT (K)	CRI Ra
10	0.4010	0.4020	3681	85.3
20	0.3927	0.4015	3797	83.8
30	0.3879	0.4066	4020	80.2
40	0.3826	0.4052	4134	80.1
50	0.3782	0.4007	4219	82.5

In addition, as for the use of Eu^{2+}–Mn^{2+} based phosphors in high-power LEDs, the phosphor quenching by saturation will exist due to the high light flux incident on the phosphors in LED packages and the slow radiative relaxation rate of Mn^{2+}.[19] However, this saturation can be practically reduced or eliminated by using phosphors with shorter lifetimes or lamp designs that reduce the incident flux on Eu^{2+}–Mn^{2+} phosphors.

Conclusions

The single-phase α- and β-$Ca_2P_2O_7$:Eu^{2+}, Mn^{2+} are synthesized through solid-state reaction and the phase-dependent photoluminescent properties are investigated. α-$Ca_2P_2O_7$:Eu^{2+}, Mn^{2+} demonstrates a wide excitation spectrum covering the near-UV spectral region, exhibiting potential use for a near-UV chip LED. Luminescence and energy transfer in Eu^{2+} and Mn^{2+} codoped α-$Ca_2P_2O_7$ are studied. For Mn^{2+} in this system, there exists a luminescent quenching concentration higher than 14 mol %. The ratio of the orange emission (595 nm) to the blue (416 nm) obtained from emission spectra is consistent with the theoretical calculation based on energy transfer and lifetime measurements. The white LED fabricated through the integration of a GaN near-UV chip and two phosphor blends (α-$Ca_2P_2O_7$:Eu^{2+}, Mn^{2+} blue–orange phosphor and Ba_2SiO_4:Eu^{2+} green phosphor) into a single package shows a warm white light of 3797 K correlated color temperature, a good CRI of 84, and a luminescent efficiency of 11 lm/W with color coordinates of $x = 0.39$, $y = 0.40$. The CRI can be improved to 94 by adding blue $Ca_2(PO4)_3Cl:Eu^{2+}$ phosphor to the two phosphor blends. The

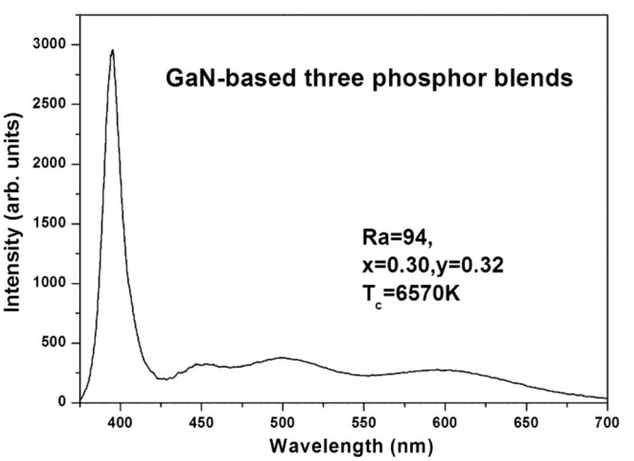

Figure 9. PL spectra of the UV-pumped white LED with the blend phosphors of $Ca_2(PO4)_3Cl$:0.02Eu^{2+} α-$Ca_2P_2O_7$:0.04Eu^{2+}, 0.12Mn^{2+} and Ba_2SiO_4:0.03Eu^{2+} under the forward-bias currents of 20 mA.

present paper demonstrates α-$Ca_2P_2O_7$:Eu^{2+}, Mn^{2+} to be a promising phosphor with an intense orange component for white LEDs.

Acknowledgment

This work is financially supported by the MOST of China (2006CB601104, 2006AA03A138), and by the National Natural Science Foundation of China (10774141, 10574128).

Chinese Academy of Sciences assisted in meeting the publication costs of this article.

References

1. Y. Narukawa, I. Niki, K. Izuno, M. Yamada, Y. Murazaki, and T. Mukai, *Jpn. J. Appl. Phys., Part 2*, **41**, L371 (2002).
2. N. Lakshminarasimhan and U. V. Varadaraju, *J. Electrochem. Soc.*, **152**, H168 (2005).
3. J. S. Kim, P. E. Jeon, J. C. Choi, H. L. Park, S. I. Mho, and G. C. Kim, *Appl. Phys. Lett.*, **84**, 2931 (2004).
4. C. H. Kuo, J. K. Sheu, S. J. Chang, Y. K. Su, L. W. Wu, J. M. Tsai, C. H. Liu, and R. K. Wu, *Jpn. J. Appl. Phys., Part 1*, **42**, 2284 (2003).
5. W. Ding, J. Wang, M. Zhang, Q. Zhang, and Q. Su, *J. Solid State Chem.*, **179**, 3394 (2006).
6. W. J. Ding, J. Wang, M. Zhang, Q. H. Zhang, and Q. Su, *J. Solid State Chem.*, **179**, 3394 (2006)
7. A. Doat, F. Pellé, and A. Lebugle, *J. Solid State Chem.*, **178**, 2354 (2005).
8. W. M. Yen and M. J. Weber, *Inorganic Phosphor*, p. 94, CRC Press, New York (2004).
9. Z. D. Hao, J. H. Zhang, X. Zhang, X. Y. Sun, Y. S. Luo, and S. Z. Lu, *Appl. Phys. Lett.*, **90**, 261113 (2007).
10. M. Zhang, J. Wang, Q. Zhang, W. Ding, and Q. Su, *Mater. Res. Bull.*, **42**, 33 (2007).
11. B. Henderson and G. F. Imbusch, *Optical Spectroscopy of Inorganic Solids*, Clarendon Press, Oxford (1989).
12. N. C. Webb, *Acta Crystallogr.*, **21**, 942 (1966).
13. C. Calvo, *Inorg. Chem.*, **7**, 1345 (1968).
14. W.-J. Yang, L. Luo, T.-M. Chen, and N.-S. Wang, *Chem. Mater.*, **17**, 3883 (2005).
15. M. M. Broer, D. L. Huber, W. M. Yen, and W. K. Zwicker, *Phys. Rev. Lett.*, **49**, 394 (1982).
16. M. Inokuti and F. Hirayama, *J. Chem. Phys.*, **43**, 1978 (1965).
17. J. S. Kim, P. E. Jeon, W. N. Kim, J. C. Choi, H. L. Park, and G. C. Kim, *Mater. Res. Soc. Symp. Proc.*, **817**, L9.4.1 (2004).
18. A. M. Srivastava, H. A. Comanzo, and A. A. Setlur, U.S. Pat. No. 6,616,862 (2003).
19. A. A. Setlur, J. J. Shiang, and U. Happek, *Appl. Phys. Lett.*, **92**, 081104 (2008).